

Melt flow behaviour of poly- ϵ -caprolactone in fused deposition modelling

H. S. Ramanath · C. K. Chua · K. F. Leong ·
K. D. Shah

Received: 23 February 2007 / Accepted: 5 June 2007 / Published online: 10 July 2007
© Springer Science+Business Media, LLC 2007

Abstract Fused deposition modelling (FDM) is an extrusion based Rapid prototyping (RP) technique which can be used to fabricate tissue engineering scaffolds. The present work focuses on the study of the melt flow behaviour (MFB) of Poly- ϵ -caprolactone (PCL) as a representative biomaterial, on the FDM. The MFB significantly affects the quality of the scaffold which depends not only on the pressure gradient, its velocity, and the temperature gradients but also physical properties like the melt temperature and rheology. The MFB is studied using two methods: mathematical modelling and finite element analysis (FEA) using Ansys®. The MFB is studied using accurate channel geometry by varying filament velocity at the entry and by varying nozzle diameters and angles at the exit. The comparative results of both mathematical modelling and FEA suggest that the pressure drop and the velocities of the melt flow depend on the flow channel parameters. One inference of particular interest is the temperature gradient of the PCL melt, which shows that it liquefies within 35% of the channel length. These results are invaluable to better understand the MFB of biomaterials that affects the quality of the scaffold built via FDM

and can also be used to predict the MFB of other biomaterials.

Introduction

Rapid prototyping (RP) is extensively researched for the fabrication of tissue engineering scaffolds [1–3]. RP can be classified under three broad headings based on the type of raw material used, namely, solid, liquid and powder based [4]. Fused Deposition Modelling (FDM) is an extrusion RP technique which uses build materials in a solid filament form. The FDM machine used for this study is the FDM 3000. Though the FDM extrusion head is designed to use Acrylonitrile butadiene styrene (ABS), many researchers have investigated the use of biomaterials such as PCL, for scaffold fabrication [1, 5–9]. Products made from PCL have been approved by the Food and Drug Administration (FDA). PCL is a semi-crystalline biodegradable polyester. Due to PCL's excellent biocompatibility it is being investigated and applied in many biomedical applications including scaffolds for tissue engineering [6, 7, 9–16].

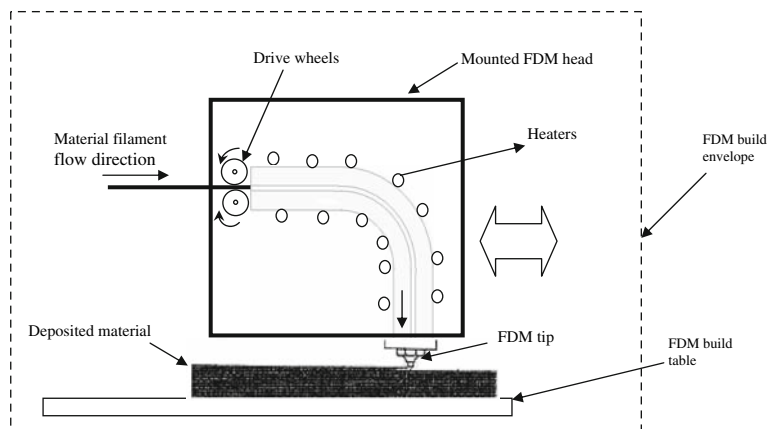
The FDM is a versatile process as it is able to handle different materials even though it requires the material to be in a solid filament form. The FDM has the ability to fabricate complex 3D scaffold geometries using layer by layer deposition technique by integrating computer aided design (CAD), polymer science, computer numerical control, and extrusion technologies [4]. The sectional view of the FDM head is shown in Fig. 1. In the FDM, the filament of diameter 1.78 mm is fed via motorised drive wheels in to a heated FDM extrusion head where it is melted.

H. S. Ramanath (✉)
Singapore Institute of Manufacturing Technology,
Singapore 638075, Singapore
e-mail: ramanath@simtech.a-star.edu.sg

C. K. Chua · K. F. Leong
School of Mechanical and Aerospace Engineering, Nanyang
Technological University, Singapore 639798, Singapore

K. D. Shah
School of Mechanical and Building Sciences, Vellore Institute of
Technology, Vellore, India

Fig. 1 Sectional view of the FDM extrusion head showing the melt flow channel and the process of extrusion [17]



The extrusion head is maintained at a temperature slightly above the melting point of the filament material. The solid filament entering the extrusion head acts as a piston to push the molten material in the extrusion channel towards the exit. The extrusion head is mounted on a movable stage, which can traverse in the x - y plane, remains in a thermally controlled build chamber. The extrudate at the exit tip is laid in a predefined pattern as a “road”, layer by layer, which solidifies almost immediately. The scaffold is completed by moving FDM build table in z axis downwards by predetermined thickness after every layer. The scaffold quality built via the FDM is thus dependent on the size of the roads, the shape, the uniformity and consistency of the roads.

For the FDM, the melt flow channel’s shape and the length are designed for ABS in a standard FDM extrusion head. It is of particular interest to determine what happens in the melt flow channel when the filament material is changed to PCL. The flow behaviour of the PCL melt is influenced by the pressure drop, velocity, the length of the channel and also the geometrical form and dimensions at the exit. The pressure drop along the melt flow channel directly influences the force required to push the filament. However, the force applied on to the filament via drive wheels is constant irrespective of the pressure drop along the channel as the current FDM system does not have a pressure drop feedback system. Hence, when the pressure drop varies, the road widths of the scaffold vary and hence vary its quality. Therefore determining the force required is crucial as it paves the way for calculating the motor power required to push the filament through the melt flow channel [18, 19]. The other parameter of significance is the channel length necessary to change the solid filament into a melt which is dependent on the rheological property of the PCL. In a wider perspective, determining the channel length is important for thermally sensitive materials which may degrade if they are left longer in the melt flow channel and it may eventually affect the quality of the scaffold fabricated.

A generic mathematical model and a FEA simulation model are proposed so as to better understand the melt flow behaviour (MFB) of PCL in the melt flow channel. The MFB characteristics considered for this study are pressure drop, velocity and temperature variations for PCL melt along the flow channel.

Materials and methods

To investigate the MFB of PCL, experiments were conducted to determine the FDM machine parameters, thermal and rheological properties of PCL. A geometrical model of the melt flow channel was built to develop a mathematical model and carry out FEA.

FDM machine parameters

The FDM machine parameters that affect the melt flow are the build chamber temperature, the volumetric rate of material flow in to the extrusion head and the temperature of the extrusion head. Consistency and magnitude of these parameters are vital in building a quality scaffold. The build chamber temperature was measured using a K type thermocouple at five positions A, B, C, D and E on the FDM build table as shown in Fig. 2, at two positions of the FDM head. From the experiments it was found that the best suited chamber temperature range was between 40 °C and 45 °C which is when the variations at five locations were within 1 °C deviation.

The volumetric material flow rate determines the rate at which the solid filament becomes fluidic in the melt flow channel. The volume flow rate was measured by measuring the feed rate of the PCL filament in to the extrusion head which also determines the inlet velocity of the filament. This measurement was based on a fixed extrusion time of two minutes and the material extruded was weighed at the exit of the extrusion head, upon which the volumetric flow rate was calculated. Entry and exit diameters considered

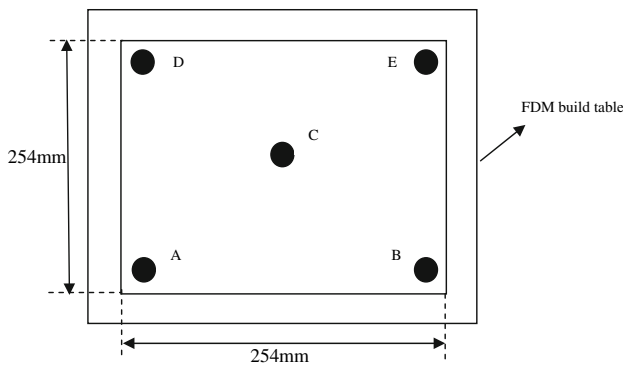


Fig. 2 Plan view of the FDM build table showing the five positions (A, B, C, D and E) for measuring temperature (Not to scale)

for the melt flow channel were 1.8 mm and 0.3 mm, respectively. Table 1 shows the measured and calculated data for two trials from which the entry velocity of the PCL filament in to the extrusion head was found to be 0.0011 m/s.

Geometric modelling of the melt flow channel

Good mathematical modelling and FEA of flow behaviour depends on the accuracy of the geometry considered for analysis. Hence, to determine the exact profile of the melt flow channel, X-ray scanning was carried out to obtain the internal features of the extrusion head. From the X-ray scan it was observed that the cross section of the melt flow channel is cylindrical with uniform cross section. Figure 3

shows the sectional view of the melt flow channel. To aid the mathematical modelling and FEA the melt flow channel was divided in to five zones. Zones 1, 2 and 3 are cylindrical in cross section however zone 4 is conical as shown in detail D. Zone 5 is cylindrical and is located at the exit of the melt flow channel.

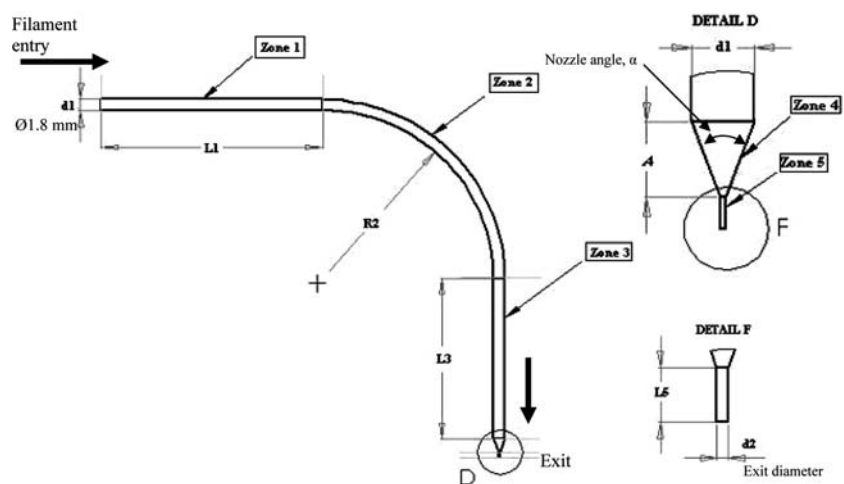
Physical properties of PCL

The values of the physical properties of PCL such as its melting temperature, thermal conductivity, rheology and specific heat are essential to investigate the MFB. The melting temperature of PCL of molecular weight 20000, supplied by Polysciences Inc., was measured using a differential scanning calorimeter (TA Instruments, DSC 2920) and was found to be 57.17 °C. Thermal conductivity of PCL was tested using the C-MATIC[®] thermal conductance tester on two samples of diameter 50 mm with thicknesses 6 mm and 4.1 mm at 75 and 67.5 °C, respectively. The thermal conductivity was found to be 0.203 W/ m K. The rheological behaviour of PCL was studied using the CSL² 500 Carri-Med Rheometer (TA instruments Inc.). Rheology experiments were conducted on PCL samples between temperatures 50 and 100 °C in steps of 5 °C. Figure 4 shows the plot of viscosity versus shear rate of PCL measured with a sample of diameter 20 mm and thickness 0.2 mm at 75 °C. The melt flow shear rate of PCL changed rapidly up to a temperature of 100 °C exhibiting pseudo plastic behaviour [20, 21]. Based on the

Table 1 Inlet and exit velocity of the extrusion head

| Trial No. | Time (s) | Measured weight of material collected at the exit (g) | Calculated volume flow rate (m ³ /s) | Calculated entry velocity, V ₁ (m/s) | Calculated exit velocity, V ₂ (m/s) |
|-----------|----------|---|---|---|--|
| 1 | 120 | 0.367 | 2.671E-09 | 0.00110 | 0.08502 |
| 2 | 120 | 0.369 | 2.6856E-09 | 0.00110 | 0.08548 |

Fig. 3 Sectional view of the melt flow channel showing the five zones considered for simulation, filament entry and exit area



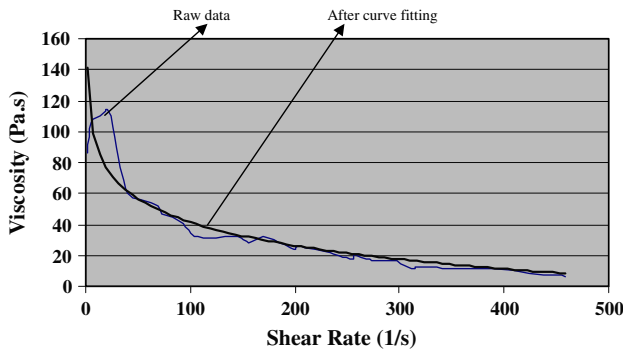


Fig. 4 Viscosity versus shear rate for PCL sample at 75 °C with a sample thickness of 0.2 mm

rheology experimental results for PCL, power law index, n , was found to be 0.42, clearly indicating a pseudo-plastic or shear-thinning behaviour, which is typical of polymeric fluids and melts [22, 23]. Based on these results, power law for non-Newtonian fluid was used for modelling the flow behaviour of PCL melt even though in FDM the liquefier extrudes a “semi-liquid” filament, not a molten liquid.

Variables considered for simulation

The variables of the melt flow channel that were considered for the simulation study are the filament entry velocity, V , nozzle angle, α , and the nozzle exit diameter, d_2 . Nozzle angle and exit diameters are in the zones 4 and 5 respectively (see Fig. 3). Filament entry velocity variation has been considered from 0.0011 m/s to 0.020 m/s. The FEA was conducted by considering five nozzle angles of 20°, 30°, 40°, 50°, 60° and the three nozzle exit diameters considered were 0.25, 0.3 and 0.4 mm. The other three zones, 1–3, have a uniform cross sectional area and are not considered as variables for FEA simulation.

Mathematical modelling

Mathematical model of the melt flow channel was derived using power law for non Newtonian polymer melt flow [22] which is:

$$\dot{\gamma} = \phi \tau^m \tag{1}$$

where $\dot{\gamma}$ is the shear rate, ϕ is the fluidity, m is the flow exponent and τ is the shear stress. The melt flow channel was divided into five zones as shown in the Fig. 3.

Power law is also expressed as:

$$\eta = K \dot{\gamma}^{n-1} \tag{2}$$

where K is the consistency index and n is the power law index [23].

Using the Eq. 1 the pressure drops ΔP_1 to ΔP_5 for five zones (refer Fig. 3) were derived by considering a steady state isothermal process in the melt flow channel based on the initial work done by Bellini [18]. They are as follows:

$$\Delta P_1 = 2L_1 \left(\frac{V}{\phi}\right)^{\frac{1}{m}} \left(\frac{m+3}{r_1^{m+1}}\right)^{\frac{1}{m}} \exp \left[\alpha \left(\frac{1}{T-T_0} - \frac{1}{T_x-T_0} \right) \right] \tag{3}$$

$$\Delta P_2 = 2L_2 \left(\frac{V}{\phi}\right)^{\frac{1}{m}} \left(\frac{m+3}{r_1^{m+1}}\right)^{\frac{1}{m}} \exp \left[\alpha \left(\frac{1}{T-T_0} - \frac{1}{T_x-T_0} \right) \right] \tag{4}$$

$$\Delta P_3 = 2L_3 \left(\frac{V}{\phi}\right)^{\frac{1}{m}} \left(\frac{m+3}{r_1^{m+1}}\right)^{\frac{1}{m}} \exp \left[\alpha \left(\frac{1}{T-T_0} - \frac{1}{T_x-T_0} \right) \right] \tag{5}$$

$$\Delta P_4 = \frac{2m}{3 \tan \left(\frac{\alpha}{2}\right)} \left(\frac{1}{r_2^{\frac{3}{m}}} - \frac{1}{r_1^{\frac{3}{m}}}\right) \left(\frac{V}{\phi}\right)^{\frac{1}{m}} \left[r_1^2 2^{m+3} (m+3) \right]^{\frac{1}{m}} \exp \left[\alpha \left(\frac{1}{T-T_0} - \frac{1}{T_x-T_0} \right) \right]$$

$$\Delta P_5 = 2L_5 \left(\frac{V}{\phi}\right)^{\frac{1}{m}} \left[\frac{r_1^2 (m+3)}{r_2^{m+3}} \right]^{\frac{1}{m}} \exp \left[\alpha \left(\frac{1}{T-T_0} - \frac{1}{T_x-T_0} \right) \right] \tag{7}$$

where L_1 – L_3 and L_5 are the lengths of respective zones, $L_2 = (\pi(R_2 + d_1/2))/2$, R_2 is the radius of the channel at zone 2 (refer Fig. 3), r_1 is the radius of the cylindrical area of the melt flow channel, r_2 is the exit radius, α is the nozzle angle. V is the filament velocity at the entry, ϕ is the fluidity, m is the flow exponent, T is the working temperature, T_x is the temperature at which m and ϕ are calculated, and T_0 is the absolute temperature.

Total pressure drop

The total pressure drop, ΔP , in the melt flow channel is the summation of the pressure drops across the five zones,

$$\Delta P = \Delta P_1 + \Delta P_2 + \Delta P_3 + \Delta P_4 + \Delta P_5 \tag{8}$$

Of the five zonal pressure drops, ΔP_4 and ΔP_5 are of particular interest as they depend on the cross sectional

areas in zone 4 and zone 5, which can be varied by changing the nozzle angle, α , and nozzle diameter, d_2 . By changing these two variables (i.e., α and d_2) one can study the pressure drops, MFB and flow directions. Knowing the total pressure drop, ΔP , the compression force, F , applied to the filament in order to extrude the material can be calculated as,

$$F = \Delta P \times A \tag{9}$$

where A is the cross section of the filament entry area.

The force applied, F , directly influences the amount of material extruded. As the current FDM system lacks a pressure drop feedback system, the force applied on to the filament via drive wheels is kept constant irrespective of the pressure drops. Hence, when the pressure drops vary, the road widths of the built scaffold will also vary accordingly and hence the quality of build is compromised. Therefore computing the force, F required, is crucial as it paves way to determine the motor power necessary to push the filament to obtain good quality build.

Finite element analysis modelling

To conduct FEA, the geometric models, both 2D and 3D are developed, based on the X-ray scanned data of the melt flow channel (see Fig. 3) using the Ansys®, FEA software. Figure 5 shows the 2D FEA model of the melt flow channel. Mapped meshing was employed so as to have a better control over the mesh quality. Fluid141 and Fluid142 elements [24] were studied for meshing the melt flow channel in 2D and 3D respectively. The materials considered for fluid in the channel and melt flow body were PCL and Aluminium alloy respectively. As previously explained, from the experiments for PCL, the data for its melting temperature, thermal conductivity and specific heat varying with temperature were specified. Similarly, the physical properties such as the thermal conductivity and the specific heat for the Aluminium alloy for the melt flow body were specified [25].

Fig. 5 2D FEA meshed model of the melt flow channel

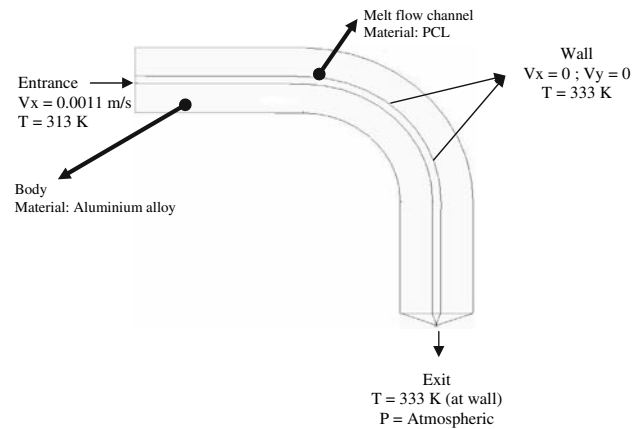
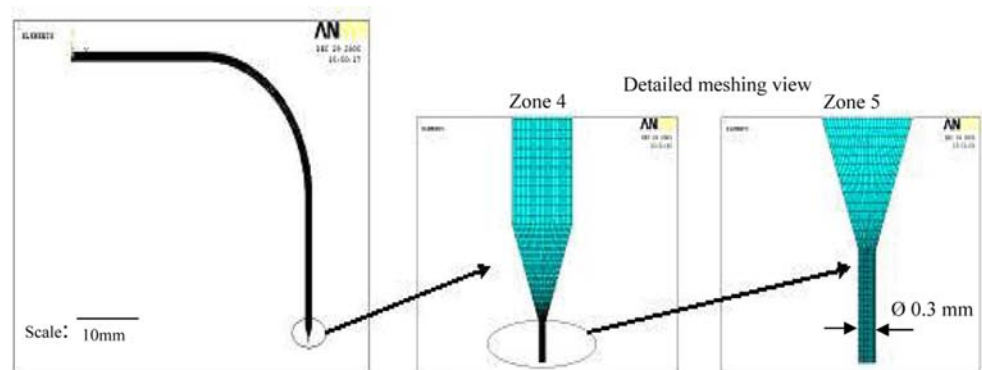


Fig. 6 Boundary conditions considered for FEA

Boundary conditions and analysis

The boundary conditions specified to conduct FEA are shown in Fig. 6. FEA was performed considering a steady state fully formed flow condition and Flotran analysis was carried out on 2D (see Fig. 5) and 3D FEA model. It was assumed that the set temperature of the FDM liquefier stays constant and extrusion process occurs slowly enough to allow the system to continually adjust to the temperature of the liquefier through heat exchange such that the extrusion process is isothermal in nature. Though in practice the process of extrusion in FDM is usually intermittent, for simplicity, it was assumed to be in the steady state and there is no change in the flow profile with time. The filament was fed at a rate of 0.0011 m/s into the melt flow channel in the x direction (see Fig. 6). However, the velocity components at the wall of the channel were assumed to be zero as the melt is assumed to be adhering to it. The temperatures at the wall and the entrance of the extrusion head were considered to be 333 K (slightly above melting point of PCL) and 313 K (FDM build chamber temperature) respectively. FEA was carried out iteratively by for varying nozzle angles and nozzle diameters, while considering the nozzle angle, $\alpha = 40^\circ$ and nozzle diameter

0.3 mm as a standard model. The number of iterations was set to obtain a converged result of the FEA.

Results and discussions

The results of mathematical modelling and FEA carried out with varying filament entry velocity, V , nozzle angle, α , and the nozzle exit diameter, d_2 , are explained in the following sections. The three characteristics of the PCL MFB that were studied are the temperature distribution, the pressure drop and the fluid velocity along the melt flow channel.

Temperature distribution along the melt flow channel

Figure 7 shows the temperature distribution plot along the melt flow channel for PCL obtained by FEA on Ansys®. The PCL melt temperature rises from 313 K to 333 K within a distance of around 42 mm from the entrance and remains constant further down along the channel. This result clearly shows that the length of the melt flow channel required for PCL is just around 35% of the total length available on a standard FDM extrusion head. As such the FDM head is over sized for PCL. As mentioned earlier, the FDM extrusion head is designed to handle materials such as ABS whose physical properties such as rheology, melt temperature are significantly higher than that of PCL.

Pressure drop along the melt flow channel

The pressure drop FEA was performed for an isothermal process under the following two cases:

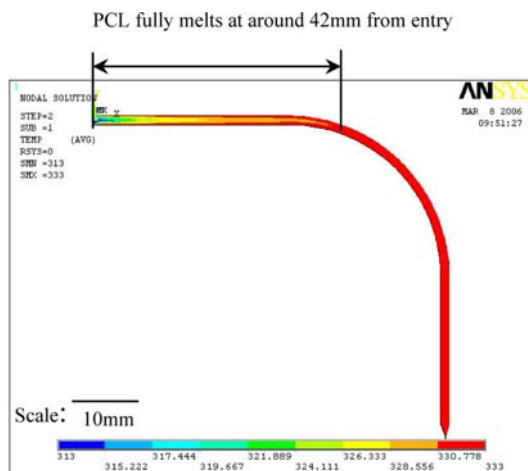


Fig. 7 Temperature distribution plot for PCL along melt flow channel

Case 1: Varying entry velocity, with the nozzle angle, $\alpha = 40^\circ$ and a nozzle diameter, $d_2 = 0.3$ mm (standard configuration).

Case 2: Constant filament entry velocity with varying nozzle angle, α and nozzle diameter, d_2 .

Case 1

The result of FEA on pressure drop variation is shown in Fig. 8. A maximum pressure of $1.64 \text{ E}+06 \text{ N/m}^2$ was found at the entrance of the melt flow channel and the pressure drops to atmospheric at the exit of the liquefier (see Fig. 6), which concurs with the initial assumption.

Case 2

The pressure drops were obtained for three nozzle diameters, 0.25, 0.3 and 0.4 mm. For each of these cases, the nozzle angles were set at 20° , 30° , 40° , 50° , and 60° . From Fig. 9 one can observe that the total pressure drop falls gradually as the nozzle angle is increased from 20° to 60° .

It can be observed from the Fig. 9 that the pressure drop is higher when nozzle diameter is smaller and less pressure drop is observed when the nozzle diameter is higher. One other observation is that the pressure drop trends for all the three diameters are similar and for any given nozzle angle, the pressure drop is higher when the nozzle diameter is small.

Results of pressure drop calculation

Comparative results of the pressure drops obtained from the mathematical modelling as well as FEA are shown in the Fig. 10. The pressure drop results shown are for standard nozzle diameter of 0.3 mm with the nozzle angle varying from 20° to 60° . The pressure drop trend lines are similar in both mathematical and FEA, though the magnitudes of the pressure drop differ which can be attributed to the FEA simulation parameters such as number and size of meshing, number of iterations and the algorithm used for solving the complex MFB.

Velocity along the melt flow channel

Figure 11 shows the FEA results for the velocity gradient and profiles along different zones of the melt flow channel for PCL with a standard nozzle diameter of 0.3 mm and a nozzle angle of 40° . The velocity profiles indicate smooth flow along the flow channel, particularly in zone 4 and 5. The velocity of the PCL melt was higher at the centre of the channel than at the walls, as the melt at the walls are assumed to be stationary. When the nozzle angles were

Fig. 8 Plot of pressure distribution along the melt flow channel for PCL under Case 1

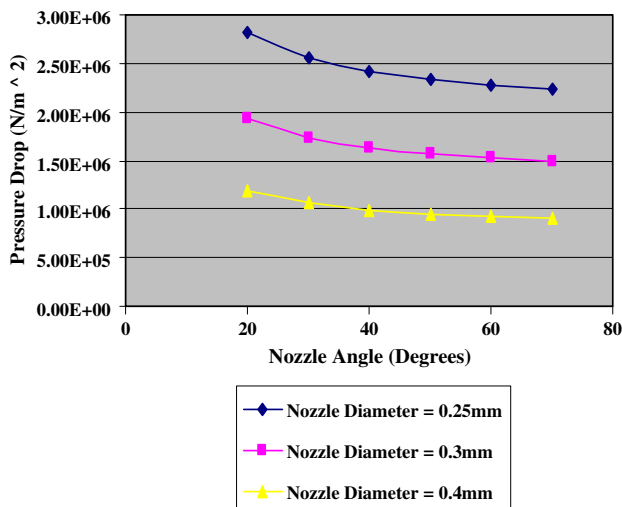
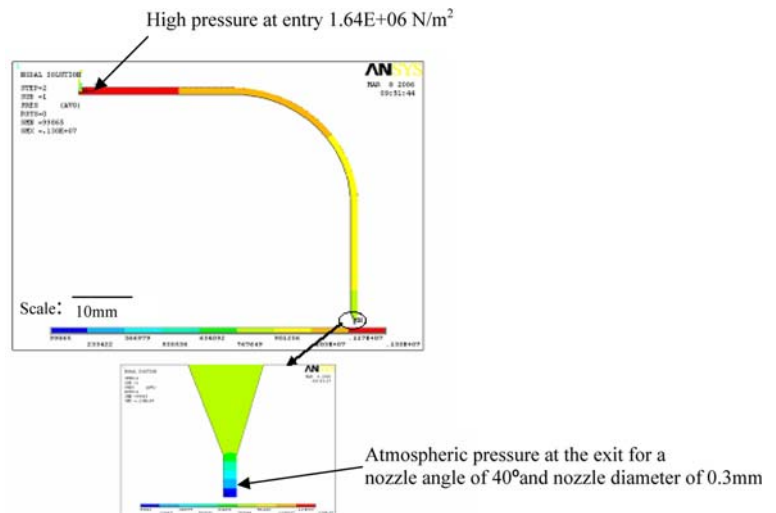


Fig. 9 Comparison of pressure drops with varying nozzle angle and nozzle diameter obtained from mathematical modelling under Case 2

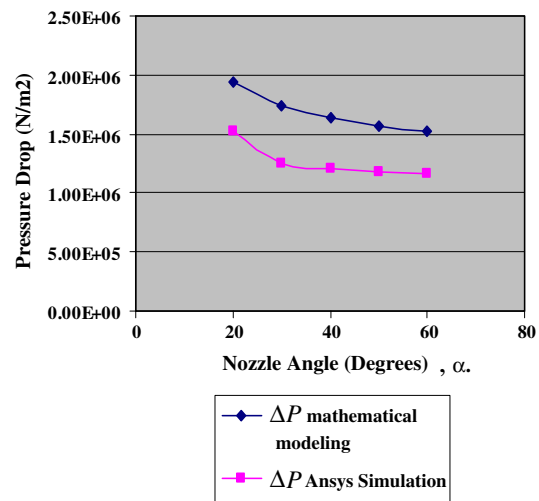


Fig. 10 Comparison of pressure drop results of mathematical modelling and FEA simulation for a fixed nozzle diameter of 0.3 mm with varying nozzle angle

varied from 20° to a maximum of 60°, the velocity profiles were similar and no back flow of the melt was observed at the zone 4. A similar result was found when the nozzle exit diameters were changed to 0.25 and 0.4 mm. For a standard configuration with nozzle diameter of 0.3 mm and nozzle angle 40°, the magnitude of the fluid velocity at the exit was found to be 0.009631 m/s, which is in good agreement with the mathematical modelling.

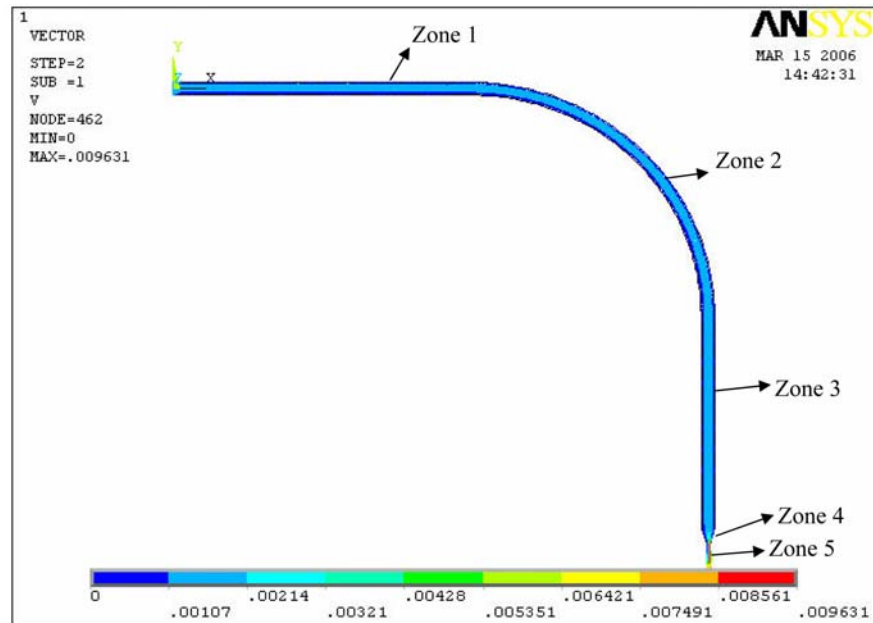
Automation of FEA

There are many variables to be analysed during the FEA simulation such as nozzle angle, nozzle diameter and the inlet velocity, not forgetting the physical properties of materials that are intended to be used such as, PCL, PLLA/PCL and Poly(glycolic acid). The FEA procedure can be

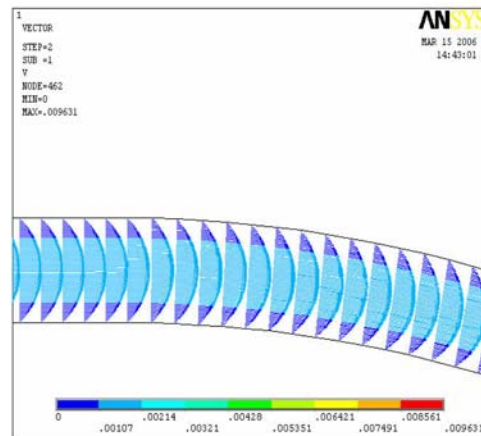
time consuming and laborious. To ease the process of FEA for these materials, a user friendly interface has been developed using visual basic 6.0 (VB). Figure 12 shows the graphical user interface (GUI) thus developed.

Using this interface, the FEA can be carried by specifying the geometry with nozzle angle and diameters, physical properties of specific material to be analysed such as the thermal conductivity, the specific heat and the melting point. The boundary conditions can be specified including the convergence criteria, number of iterations, entry velocity, temperature and pressure. An Ansys® readable text file is generated once all the necessary information is filled in this interface and simulation can then be carried out. The generic GUI developed in this work opens up the possibility of analysing and simulating the flow behaviour of many other materials even before

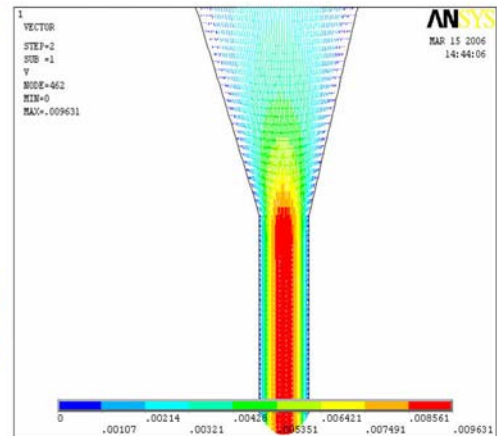
Fig. 11 (a) Velocity profiles at different zones along the melt flow channel for a standard nozzle diameter of 0.3 mm and nozzle angle 40°, (b) Velocity profile at Zone 2, (c) Velocity profiles at Zones 4 and 5



(a) Velocity profiles along liquefier channel



(b) Zone 2



(c) Zones 4 and 5

verification on the FDM. This will lead to optimal parameters that affect the MFB be determined more rapidly and to the eventual fabrication of good quality scaffold on the FDM.

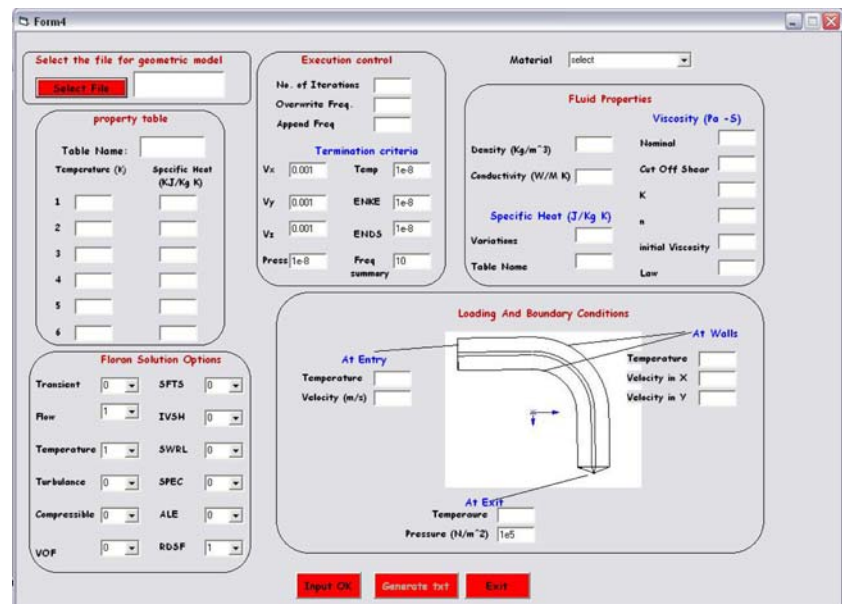
Conclusion

In conclusion, the melt flow behaviour (MFB) of PCL in the melt flow channel of the FDM has been investigated by studying the thermal behaviour, pressure drops and the velocity gradients. Two modes were employed to study the MFB, one by mathematical modelling and the other via FEA, using Ansys[®]. Key parameters that affect the MFB and essential for simulation are FDM machine parameters and physical properties of PCL. Experiments were carried

out to determine the FDM machine parameters and the physical properties like thermal conductivity, specific heat, viscosity and shear thinning property for PCL. A geometric model, based on an X-ray scan, of the melt flow channel was built to carry out the simulation. The FEA boundary conditions that represent the realistic conditions were carefully chosen for the simulation. A summary of the work along with salient conclusions arising from this study is presented in the following sections.

- A mathematical model, using power law, of the melt flow channel has been developed considering the pressure drop at the identified five zones. The summation of the zonal pressure drops has been used to calculate the force required to feed the filament as the force applied on the filament directly influences the amount of material extruded. The FEA results showed a

Fig. 12 Graphical user interface (GUI) showing details of input parameters for FEA



maximum pressure of $1.64\text{E}+06 \text{ N/m}^2$ at the entrance of the melt flow channel and this concurred with the mathematical modelling. The pressure drops at five zones were obtained for three nozzle diameters, 0.25, 0.3 and 0.4 mm by varying the nozzle angles from 20° , 30° , 40° , 50° and 60° . The mathematical and simulation results concurred that the nozzle diameter and angle variation has a direct effect on pressure drop along the melt flow channel and both the results showed a similar pressure drop trend lines.

- Relationship between pressure drop and the force required to push the filament has been established in this study. However, the FDM extrusion head considered here do not have a pressure drop feedback system; hence the force applied on to the filament via drive wheels is constant irrespective of the pressure drops. The implication of this observation is that when the pressure drops vary, the road widths of the scaffold will also vary, thus affecting the quality and consistency of the scaffold built.
- The thermal behaviour simulation results showed that the PCL fully melts at about 42 mm from the entry. This result indicates that the standard melt flow channel of FDM is oversized in terms of the channel length for the PCL material, resulting in a longer stay for the PCL melt in the molten state before leaving the extrusion head.
- The velocity profiles showed smooth flow along the flow channel, in particular in zone 4 and 5. The velocity of the PCL melt was higher at the centre of the channel than at the walls, as the melt at the walls are assumed to be stationary. No material back flow was observed at the zone 4 when the nozzle angles were changed to 20° , 30° , 40° , 50° or 60° .

The MFB of PCL has been studied and findings are significant which are useful in understanding and optimising the FDM parameters. To automate the process of FEA, a GUI has been developed which can be used to determine the MFB of other materials in the melt flow channel especially those of biomaterials. Based on the findings of this study, further work will be carried out to study the MFB of PCL/Hydroxyapatite composites, PLLA/PCL and other biomaterials, which can be used in FDM to fabricate tissue scaffolds.

References

1. S. F. YANG, K. F. LEONG, Z. DU and C. K. CHUA, *Tiss. Eng.* **7**(6) (2001) 679
2. S. F. YANG, K. F. LEONG, Z. DU and C. K. CHUA, *Tiss. Eng.* **8**(1) (2002) 1
3. W. Y. YEONG, C. K. CHUA, K. F. LEONG and M. CHANDRASEKARAN, *Trend Biotechnol.* **22**(12) (2004) 643
4. C. K. CHUA, K. F. LEONG and C. S. LIM, *Rapid Prototyping, Principles and Applications*, 2nd edn. (World Scientific Publishing Co.Pte Ltd, Singapore, 2003)
5. K. F. LEONG, C. M. CHEAH and C. K. CHUA, *Biomaterials* **24**(13) (2003) 2363
6. M. H. TOO, K. F. LEONG, C. K. CHUA, Z. DU, S. F. YANG, S. L. HO and C. M. CHEAH, *Int. J. Adv. Manufact. Technol.* **19**(3) (2002) 217
7. K. C. ANG, K. F. LEONG, C. K. CHUA and M. CHANDRASEKARAN, *Rapid Prototyping J.* **12**(2) (2006) 100
8. H. S. RAMANATH, M. CHANDRASEKARAN, C. K. CHUA, K. F. LEONG and K. D. SHAH, *Key Eng. Mater.* **334-335** (2007) 1241
9. K. C. ANG, K. F. LEONG, C. K. CHUA and M. CHANDRASEKARAN, *J. Biomed. Mater. Res.: Part A.* **80A**(3) (2007) 655
10. I. ZEIN, D. W. HUTMACHER, K. C. TAN and S. H. TEOH, *Biomaterials* **23** (2002) 1169

11. F. WANG, L. SHOR, A. DARLING, S. KHALIL, W. SUN, S. GUÈCÈERI and A. LAU, *Rapid Prototyping J.* **10/1** (2001) 42
12. A. L. DARLING and W. SUN, *J. Biomed. Mater. Res. Part B: Appl. Biomater.* **70B** (2004) 311
13. S. KHALIL, J. NAM and W. SUN, *Rapid Prototyping J.* **11**(1) (2005) 9
14. G. CIARDELLI, V. CHIONO, C. CRISTALLINI, N. BARBANI, A. AHLUWALIA, G. VOZZI, A. PREVITI, G. TANTUSSI and P. GIUSTI, *J. Mater. Sci.: Mater. Med.* **15** (2004) 305
15. R. C. THOMSON, M. J. YASZEMSKI, J. M. POWERS, and A. G. MIKOS, *J. Biomater. Sci.: Polym. Ed.* **7**(1) (1995) 23
16. Y. IKADA and H. TSUJI, *Macromol. Rapid Commun.* **21** (2000) 117
17. FDM 3000 system documentation Startasys Inc., USA (2001)
18. A. BELLINI, Fused deposition of ceramics: A comprehensive experimental, analytical and computational study of material behaviour, fabrication process and equipment design. PhD thesis, (Drexel University, USA, 2002)
19. K. Y. JIANG and Y. H. GU, *Key Eng. Mater.* **259–260** (2004) 667
20. M. P. GROSVENOR and J. N. STANIFORTH, *Int. J. Pharmaceut.* **135** (1996) 103
21. Z. PINGPING, Y. HAIYANG and W. SHIQIANG, *Eur. Polym. J.* **34**(1) (1998) 91
22. W. MICHAELI, *Extrusion Dies: Design and Engineering Computations*. (Hanser Publications, Munich, 1984) pp. 10
23. C. RAUWENDAAL, *Polymer Extrusion*, 3rd edn. (SPE 1994) pp. 182
24. ANSYS element reference manual, Ansys Inc., USA (2004)
25. Asm Handbook, *Properties and Selection: Nonferrous Alloys and Special-Purpose Materials Section: Volume 2*. (ASM International, USA, 1991)